Dynamic Optimization of Distributed Photovoltaic (DPV) Systems

Chenzhe Zhang

November 28, 2025

1 Introduction

Distributed photovoltaic (DPV) systems have become a key component of China's low carbon transition and rural development strategy. Unlike giant solar farms that feed into high voltage transmission grids, DPV consists of small rooftop or village level installations connected to local distribution networks (Figure 1). Since 2013, China has relied heavily on feed-in tariffs (FITs) and targeted poverty alleviation programs to stimulate DPV deployment, with subsidies starting high and then being sharply reduced as costs fell and fiscal pressure mounted.

This paper develops a continuous-time optimal control framework in which a social planner jointly chooses a DPV subsidy and a direct pollution abatement effort. Moreover, the planner internalizes learning by doing in deployment cost, the evolution of renewable capital stock, the pollution stock, and the fiscal burden of subsidizing an expanding capital base. Within this setting, we characterize the steady state and the optimal transition path, showing how a front-loaded subsidy followed by phase out can be optimal, and study how renewable deployment substitutes intertemporally for future direct abatement. We then analyze how the optimal policy responds to changes in environmental preferences, grid absorption efficiency, and market frictions.

Figure 1: DPV on rooftops

2 Policy Background and Motivation

China's distributed photovoltaic (DPV) sector has undergone a rapid shift from generous support to full subsidy phase out. The central Feed-in Tariff (FIT) started at 0.42 RMB/kWh in 2013 and remained stable for several years, but was reduced twice in 2018, followed by sharp cuts in 2019 and 2020, and was discontinued for new projects in 2021. Figure 2 summarizes this sequence.

A notable feature of this path is its clear pattern: an early stage of high and stable subsidies, followed by an accelerated decline as deployment expanded. While often described as administrative or fiscal adjustments, this pattern raises a broader question: what economic forces justify a front-loaded subsidy followed by a phase out?

Existing discussions document the policy changes but do not provide a framework that links declining FITs to declining deployment costs, pollution reduction, and the fiscal burden of supporting an expanding capital stock. These gaps motivate our central question: what is the optimal dynamic subsidy path when renewable investment and direct abatement jointly determine pollution stock and solar panel stock? Moreover, what is the substitution rate between these two policy instruments?

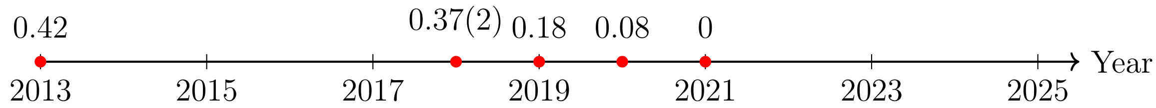

Figure 2: Subsidy Policy Change for DPV, units: RMB/kWh

3 Literature Review

This paper relates to three streams of literature. The first provides the policy context for distributed photovoltaic (DPV) deployment as a tool for rural development. The second examines how policy stability shapes the timing of investment. Finally, the most closely related stream develops dynamic optimal control frameworks for energy and environmental policy.

3.1 DPV as Development Policy

The first stream of empirical work documents the socio-economic benefits of DPV as part of China's broader rural development and poverty alleviation strategy (2013–2020). Li et al. (2025b) and Wu et al. (2025) show that targeted interventions, including DPV projects, significantly raise rural household income and reduce multidimensional poverty, with heterogeneous gains for vulnerable groups. At the macro level, Wang and Zhen (2025) use county-level panel data to show that DPV rollout reduces carbon emissions while increasing local GDP, highlighting DPV as a dual-benefit policy instrument. Micro-level studies such as Li et al. (2025a) emphasize the role of government agents, perceived benefits, and community dynamics in shaping PV adoption behavior.

These studies establish the policy importance of DPV but are largely descriptive and rely on reduced-form estimation. They do not model how an optimizing planner should design the dynamic path of subsidies and abatement. Our work fills this theoretical gap by building a structural model that embeds deployment costs, fiscal burdens, and pollution dynamics within an optimal control framework.

3.2 Policy Uncertainty and Investment Timing

The second stream of literature studies how the credibility and temporal stability of subsidy policies affect investors' timing decisions. Hagspiel et al. (2021) show that when the probability of subsidy withdrawal increases, investors delay adoption. Sendstad and Chronopoulos (2020) demonstrate that sequential investment strategies can mitigate some adverse effects of volatility. Using evidence from small hydropower, Linnerud et al. (2014) highlight heterogeneous investor responses to subsidy uncertainty, with professional investors strategically postponing investment.

This literature underscores that the temporal profile of subsidies is central to technology adoption. However, it focuses on private investors facing uncertainty and does not provide normative guidance for the social planner's optimal subsidy trajectory. Our model complements this literature by shifting the focus to the policymaker, who must not only design the optimal time path of subsidies but also address market frictions that can lead to resource misallocation.

3.3 Dynamic Optimal Control in Energy Policy

The most directly related literature applies optimal control to energy transitions. Classic models of resource depletion (e.g., Hotelling, 1931; Slade and Thille, 2009) analyze intertemporal extraction choices, while Keeler et al. (1972) formalize pollution as a stock variable requiring abatement. Chakravorty et al. (1997) integrate these traditions by combining endogenous technological learning with multi-resource substitution, showing how learning in backstop technologies alters long-run extraction behavior.

Our model builds on and extends this tradition in several ways. First, we introduce two policy instruments: renewable investment subsidies and direct abatement. This allows us to study their interaction along the transition path. Second, we incorporate learning by doing in deployment, which generates strategic incentives for early cost-reducing investment and helps rationalize front-loaded subsidy policies. Third, by treating both renewable capacity and pollution as state variables, we endogenize the long-run trade-off between stock-based and flow-based pollution management. Finally, we capture the fiscal burden arising from subsidizing an expanding capacity base, which provides a structural rationale for subsidy phase-out policies.

3.4 Link to Our Contribution

Taken together, the existing literature explains the development impacts of DPV, highlights the importance of credible subsidy policies, and establishes the analytical foundations of dynamic environmental control. What is missing is a unified framework that jointly models (i) pollution and capital stock dynamics, (ii) learning-driven cost declines, (iii) fiscal interactions in subsidy design, and (iv) the intertemporal substitution between renewable deployment and direct abatement. By filling this gap, our paper provides theoretical foundations for understanding the observed "front-loaded and phase-out" pattern in China's FIT subsidy policy and offers broader insights for renewable energy policy design in developing economies.

The relationship between these literature streams and our contribution is summarized in Figure 3.

4 Model Setup

Consider a continuous–time social planner who chooses a time–varying subsidy $i_t \geq 0$ and direct abatement effort $A_t \geq 0$ to maximize discounted social welfare. The economy accumulates renewable energy capital K_t and evolves a pollution stock P_t.

4.1 Controls, States, and Technology

Control variables:

$$i_t \geq 0 \quad \text{(renewable subsidy)}, \qquad A_t \geq 0 \quad \text{(direct pollution abatement)}.$$

State variables:

$$K_t \quad \text{(accumulated renewable installation)}, \qquad P_t \quad \text{(pollution stock)}.$$

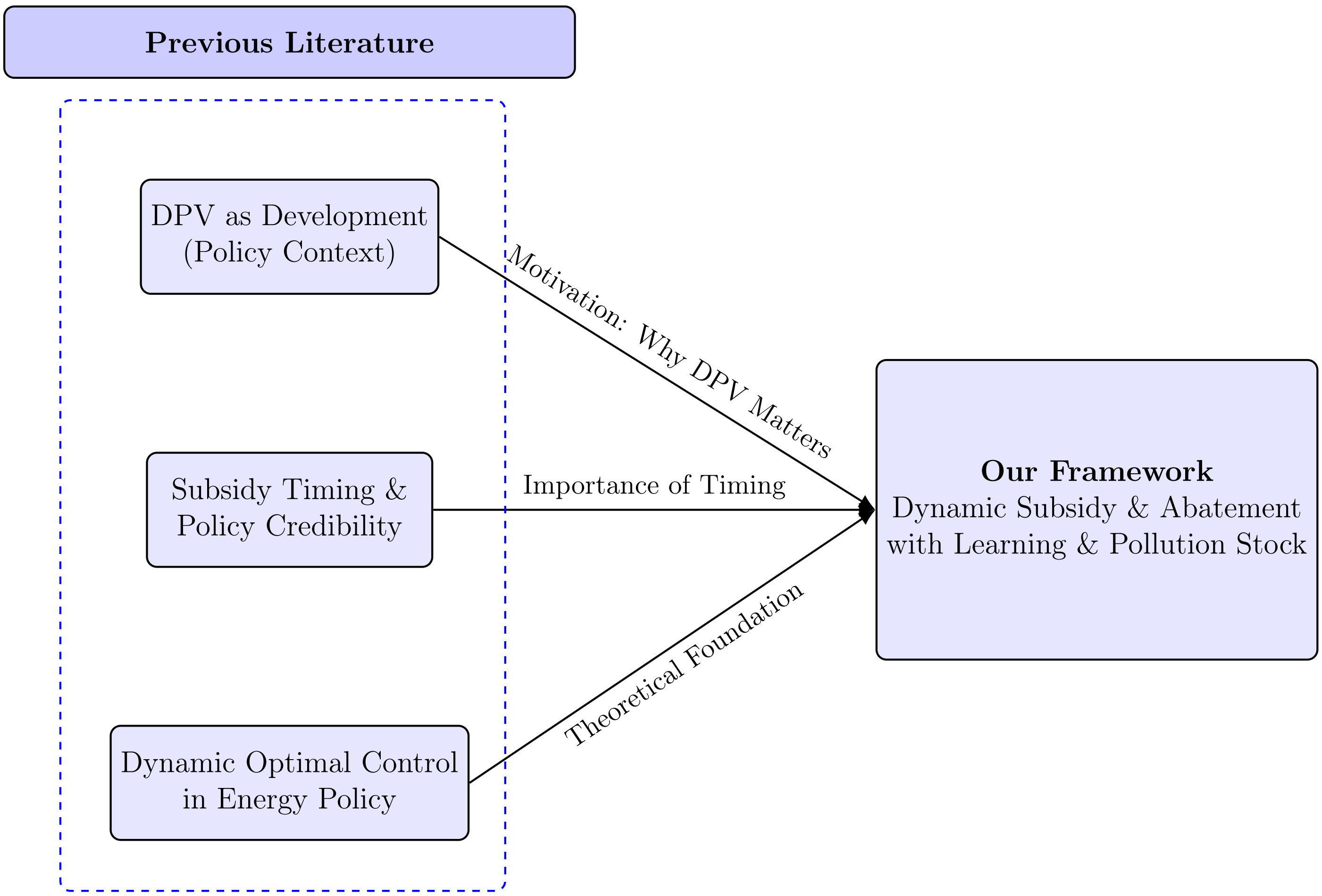

Figure 3: How the Literature Streams Connect to Our Contribution

Technology and dynamic equations:

$$u_t = a\, i_t^{\gamma}, \qquad \gamma > 0,$$

$$Q_t = \kappa K_t,$$

$$B_t = R\kappa K_t,$$

$$\dot{K}_t = u_t - \rho K_t,$$

$$\dot{P}_t = \omega - \phi P_t - \kappa K_t - A_t.$$

u_t is the induced deployment or investment at each time t. Q_t represents the clean energy generated from the panels. B_t represents some exogenous benefit for poverty alleviation. The change in the capital stock K_t is co-determined by deployment u_t and depreciation ρ. The change in the pollution stock is determined by the baseline inflow ω, natural decay ϕ, clean energy κK_t, and direct abatement A_t.

4.2 Instantaneous Payoff

We introduce another two parameters: $\eta > 0$ scales the marginal damage of pollution, while $\theta > 0$ scales the marginal cost of direct abatement. The overall instantaneous welfare is

$$\pi_t = R\kappa K_t - \eta P_t^2 - i_t \kappa K_t - \beta u_t^2 - \frac{c_0}{1+K_t} u_t - \theta A_t^2,$$

where

$$u_t = a\, i_t^{\gamma},$$

The term $\frac{c_0}{1+K_t}$ captures learning by doing in deployment cost. As cumulative deployment K_t increases, experience reduces the unit cost, but at a diminishing rate. βu_t^2 captures cost for fast deployment.

4.3 Planner's Problem

The social planner solves

$$\max_{\{i_t, A_t\}_{t\geq 0}} \int_0^{\infty} e^{-\delta t}\Big[R\kappa K_t - \eta P_t^2 - i_t\kappa K_t - \beta u_t^2 - \frac{c_0}{1+K_t}u_t - \theta A_t^2\Big]\,dt$$

5 Optimal Control Problem

5.1 Current-Value Hamiltonian

Let $(\tilde{\lambda}_K(t), \tilde{\lambda}_P(t))$ denote the current-value costate variables associated with K_t and P_t. The current value Hamiltonian is

$$\tilde{\mathcal{H}} = R\kappa K_t - \eta P_t^2 - i_t\kappa K_t - \beta u_t^2 - \frac{c_0}{1+K_t}u_t - \theta A_t^2 + \tilde{\lambda}_K(u_t - \rho K_t) + \tilde{\lambda}_P(\omega - \phi P_t - \kappa K_t - A_t),$$

with $u_t = a\, i_t^{\gamma}$.

5.2 First-Order Conditions

Subsidy i_t:

$$\frac{\partial\tilde{\mathcal{H}}}{\partial i_t} = -\kappa K_t - \left(2\beta u_t + \frac{c_0}{1+K_t}\right)\frac{\partial u_t}{\partial i_t} + \tilde{\lambda}_K\frac{\partial u_t}{\partial i_t} = 0,$$

where

$$\frac{\partial u_t}{\partial i_t} = a\gamma i_t^{\gamma-1}.$$

Equivalently,

$$\boxed{\tilde{\lambda}_K = \frac{\kappa K_t}{a\gamma i_t^{\gamma-1}} + 2\beta a i_t^{\gamma} + \frac{c_0}{1+K_t}}$$

whenever $i_t > 0$.

Direct abatement A_t:

$$\frac{\partial\tilde{\mathcal{H}}}{\partial A_t} = -2\theta A_t - \tilde{\lambda}_P = 0 \quad\Rightarrow\quad \boxed{A_t = -\frac{\tilde{\lambda}_P}{2\theta}}.$$

Costate equations: Using the current-value formulation, costate dynamics satisfy

$$\dot{\tilde{\lambda}}_K = \delta\tilde{\lambda}_K - \frac{\partial\tilde{\mathcal{H}}}{\partial K_t}, \qquad \dot{\tilde{\lambda}}_P = \delta\tilde{\lambda}_P - \frac{\partial\tilde{\mathcal{H}}}{\partial P_t}.$$

Computing derivatives yields

$$\dot{\tilde{\lambda}}_K = (\delta+\rho)\tilde{\lambda}_K - R\kappa + i_t\kappa - \frac{c_0 u_t}{(1+K_t)^2} + \kappa\tilde{\lambda}_P,$$

$$\dot{\tilde{\lambda}}_P = (\delta+\phi)\tilde{\lambda}_P + 2\eta P_t.$$

State dynamics:

$$\dot{K}_t = u_t - \rho K_t, \qquad \dot{P}_t = \omega - \phi P_t - \kappa K_t - A_t.$$

Transversality conditions:

$$\lim_{t\to\infty} e^{-\delta t}\tilde{\lambda}_K(t)K_t = 0, \qquad \lim_{t\to\infty} e^{-\delta t}\tilde{\lambda}_P(t)P_t = 0.$$

6 Steady State

If a steady state exists with $\dot{\tilde{\lambda}}_K = 0$, $\dot{\tilde{\lambda}}_P = 0$, $\dot{K}_t = 0$, $\dot{P}_t = 0$, the system converges to constant values $(K^*, P^*, i^*, u^*, A^*)$.

From $\dot{K} = 0$,

$$u^* = \rho K^*.$$

From the FOC for A_t and the costate equation for $\tilde{\lambda}_P$,

$$\tilde{\lambda}_P^* = -2\theta A^*, \qquad 0 = \dot{\tilde{\lambda}}_P^* = (\delta+\phi)\tilde{\lambda}_P^* + 2\eta P^* \quad\Rightarrow\quad -2\theta(\delta+\phi)A^* + 2\eta P^* = 0.$$

Hence

$$\boxed{A^* = \frac{\eta}{\theta(\delta+\phi)}\,P^*.}$$

The pollution stock in steady state satisfies

$$0 = \dot{P} = \omega - \phi P^* - \kappa K^* - A^* \quad \Rightarrow \quad \omega = \phi P^* + \kappa K^* + A^*.$$

Substituting the expression for A^*,

$$\omega = \phi P^* + \kappa K^* + \frac{\eta}{\theta(\delta+\phi)} P^* = \left[\phi + \frac{\eta}{\theta(\delta+\phi)}\right] P^* + \kappa K^*.$$

Solving for P^* gives

$$\boxed{P^* = \frac{\omega - \kappa K^*}{\phi + \dfrac{\eta}{\theta(\delta+\phi)}}.}$$

Using $u^* = \rho K^*$, the FOC for the subsidy implies

$$\tilde{\lambda}_K^* = 2\beta\rho K^* + \frac{c_0}{1+K^*} + \frac{\kappa K^*}{\gamma} a^{-1/\gamma} (\rho K^*)^{1/\gamma - 1}.$$

Finally, imposing $\dot{\tilde{\lambda}}_K = 0$,

$$0 = (\delta+\rho)\tilde{\lambda}_K^* - R\kappa + \kappa i^* - \frac{c_0 u^*}{(1+K^*)^2} + \kappa \tilde{\lambda}_P^*,$$

where

$$i^* = \left(\frac{\rho K^*}{a}\right)^{1/\gamma}, \qquad \tilde{\lambda}_P^* = -2\theta A^* = -\frac{2\eta}{\delta+\phi} P^*.$$

Combining all expressions, the steady state capital stock K^* is pinned down by the implicit equation

$$\boxed{F(K^*) = 0,}$$

where $F(\cdot)$ collects the terms

$$\begin{aligned} F(K) = (\delta+\rho)&\left[2\beta\rho K + \frac{c_0}{1+K} + \frac{\kappa K}{\gamma} a^{-1/\gamma} (\rho K)^{1/\gamma - 1}\right] \\ &- R\kappa + \kappa \left(\frac{\rho K}{a}\right)^{1/\gamma} - \frac{c_0 \rho K}{(1+K)^2} \;-\; \frac{2\kappa\eta}{\delta+\phi} \cdot \frac{\omega - \kappa K}{\phi + \dfrac{\eta}{\theta(\delta+\phi)}}. \end{aligned}$$

Thus, K^* solves $F(K^*) = 0$ and the remaining steady state variables follow as

$$u^* = \rho K^*, \qquad i^* = \left(\frac{\rho K^*}{a}\right)^{1/\gamma}, \qquad A^* = \frac{\eta}{\theta(\delta+\phi)} P^*, \qquad P^* = \frac{\omega - \kappa K^*}{\phi + \dfrac{\eta}{\theta(\delta+\phi)}}.$$

In the steady state, new installation u^* just offsets the depreciation ρ of the capital stock K^*, so that $u^* = \rho K^*$. The subsidy i^* is just high enough to induce this replacement investment. The optimal abatement level A^* is proportional to the steady-state pollution stock P^*: in the long run, the marginal cost of abatement (captured by θA^*) is equated to the present value of marginal pollution damages, $\frac{\eta}{\delta+\phi} P^*$. Finally, the steady-state pollution level P^* is pinned down by a flow balance condition in which the baseline inflow ω equals natural decay ϕP^* plus the contribution of clean energy κK^* and direct abatement A^*:

$$\omega = \phi P^* + \kappa K^* + A^*.$$

The implicit expression for K^* is not particularly informative term by term. The key idea is that, at K^*, the marginal benefit of an additional unit of renewable capital (through clean energy production, reduced pollution, and any exogenous poverty-alleviation benefits) exactly equals its marginal cost (including the fiscal burden of subsidies and installation costs of new panels).

7 Dynamic Substitution: Short-Run vs. Long-Run

Before presenting the numerical simulations and comparative studies, we analyze the theoretical properties of the optimal path. We distinguish between the internal dynamics of instrument substitution along a single transition path and the comparative mechanisms that generate differences across structural environments.

We begin with the internal dynamics of instrument substitution. The relationship between the two control variables, renewable investment u_t (or, equivalently, the subsidy rate i_t) and direct abatement A_t, depends on the time horizon. We focus on three time horizons: instantaneous choices at a given time t, intertemporal dynamics along the transition path, and the steady state.

At any instant t, the planner chooses i_t and A_t to satisfy

$$\tilde{\lambda}_K = \frac{\kappa K_t}{a\gamma i_t^{\gamma-1}} + 2\beta a i_t^{\gamma} + \frac{c_0}{1+K_t}, \qquad A_t = -\frac{\tilde{\lambda}_P}{2\theta}.$$

Investment responds to the shadow value of capital $\tilde{\lambda}_K$, while abatement responds to the shadow price of pollution $\tilde{\lambda}_P$. At this static margin, the two instruments are chosen independently to equate marginal benefits and marginal costs. Hence, we do not obtain any instantaneous substitution between i_t and A_t.

Over time, however, we observe intertemporal substitution. At the beginning of the transition, K_t is small, and from

$$\dot{\tilde{\lambda}}_K = (\delta+\rho)\tilde{\lambda}_K - R\kappa + i_t\kappa - \frac{c_0 u_t}{(1+K_t)^2} + \kappa\tilde{\lambda}_P,$$

the marginal value of an additional unit of K_t is high. This creates a strong incentive to set a high subsidy and induce a large investment flow u_t. According to the pollution dynamics

$$\dot{P}_t = \omega - \phi P_t - \kappa K_t - A_t,$$

a higher K_t reduces the pollution stock over time. As P_t falls, the marginal damage $|\tilde{\lambda}_P|$ decreases, and from $A_t = -\tilde{\lambda}_P/(2\theta)$, it indicates that optimal abatement A_t also declines. In this sense, we show that early investment in solar capacity reduces the need for direct abatement in later periods. Figure 4 provides a simple illustration; the corresponding calibration is reported in Table 1.

The simulated path also shows that both control variables are high at the beginning, then decline and eventually converge to low steady state levels. We interpret the decline in the subsidy as the outcome of two opposing forces. On the one hand, fiscal pressure from the flow of subsidy payments, captured by κK_t, increases with the accumulation of K_t. On the other hand, learning-by-doing, represented by the cost term $\frac{c_0}{1+K_t}$, reduces the unit cost of deployment as K_t rises. In the early stage, the learning benefit dominates and supports a high subsidy. In the later stage, fiscal pressure outweighs the incremental gains from learning-by-

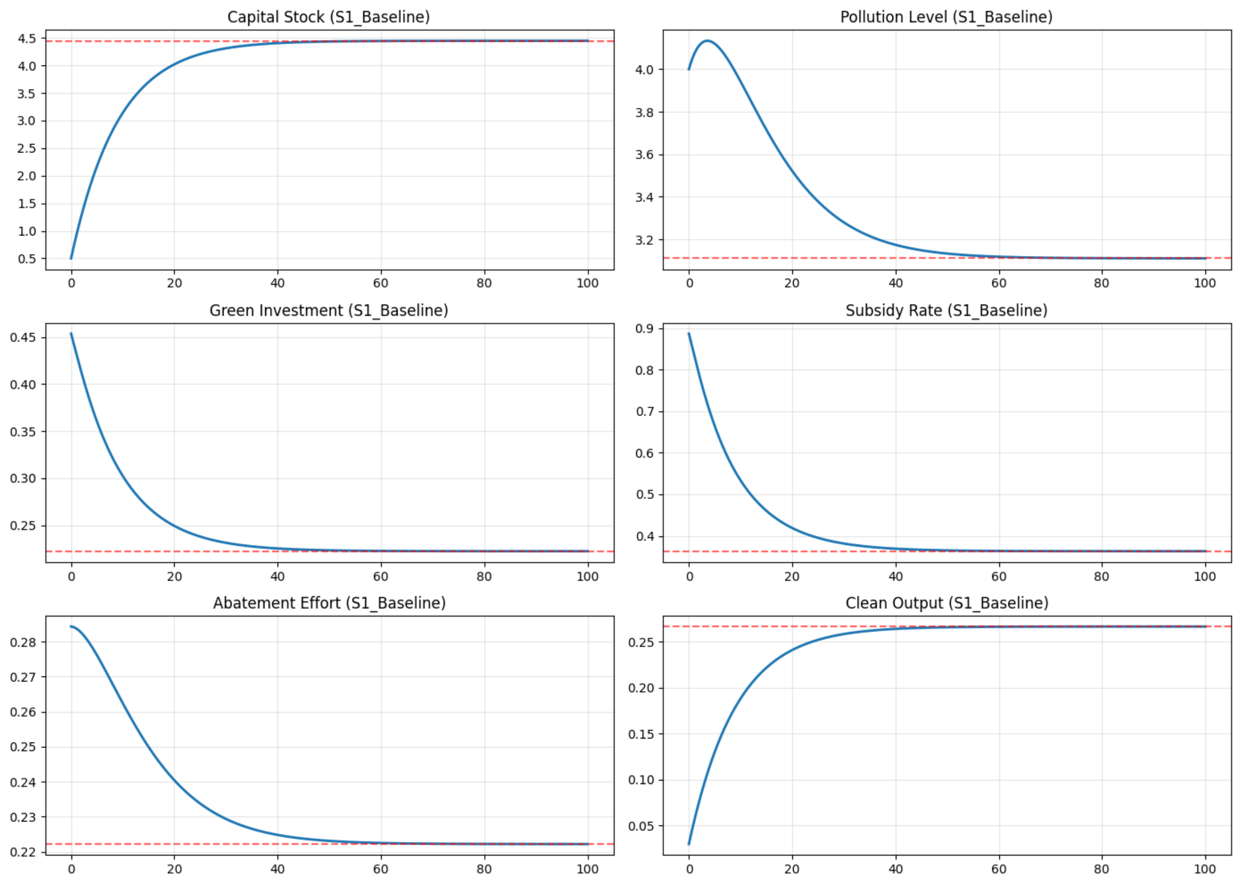

Figure 4: Baseline simulation results

doing, so the optimal subsidy rate decreases over time. Since the capital stock is not enough to decrease the pollution, the social planner also chooses a high level abatement in initial stage. Subsequently the direct abatement decreases due to the intertemporal substitution.

In the steady state, when all variables have converged to their equilibrium values, we can characterize the substitution between subsidy-induced investment and direct abatement in closed form. Combining

$$A^* = \frac{\eta}{\theta(\delta + \phi)} P^*$$

with

$$P^* = \frac{\omega - \kappa K^*}{\phi + \dfrac{\eta}{\theta(\delta + \phi)}}, \qquad u^* = \rho K^*,$$

we obtain

$$\frac{\partial A^*}{\partial K^*} = -\frac{\eta\kappa}{\phi\theta(\delta + \phi) + \eta}, \qquad \frac{\partial A^*}{\partial u^*} = -\frac{\eta\kappa}{\rho\big[\phi\theta(\delta + \phi) + \eta\big]}.$$

These expressions define the steady state substitution rate between capital (or investment) and abatement: higher K^* or u^* allows the planner to use less direct abatement A^* to maintain the same pollution stock. However, the planner does not actively adjust the controls in the steady state, because any deviation would move the system away from equilibrium.

8 Dynamic Properties and Comparative Statics

Having established the baseline optimal path, we now examine how structural parameters transmit their effects through the coupled shadow prices. These mechanisms generate predictions for how the optimal path shifts in response to structural shocks. We construct several scenarios by changing a small set of parameters while keeping the rest of the environment fixed.

To ensure comparability across scenarios, we keep the physical environment and the initial state variables constant. In all simulations, the exogenous pollution inflow ω and the natural decay rate ϕ are fixed, so the underlying natural pollution dynamics are the same. The exogenous poverty alleviation benefit R is also held constant. We initialize renewable capital at a low level and set the pollution stock at a high but feasible level, representing an economy facing a severe environmental crisis but not yet at the brink of ecological collapse. This is meant to capture the stylized conditions of the Chinese DPV market and environment around 2013.

Within this common background, we vary three dimensions that are particularly relevant for policy: (1) government preferences, by changing (η, θ), (2) solar panel effectiveness, by changing κ, and (3) market frictions in the subsidy–to–investment mapping, by changing γ. The parameter choices for the six scenarios are summarized in Table 1, and each subsection below discusses the corresponding mechanisms in more detail.

Table 1: Parameter Calibration across Scenarios

Parameter	**S1**	**S2**	**S3**	**S4**	**S5**	**S6**
Scenario Type	*Baseline*	*Strong*	*Weak*	*High Tech*	*Low Tech*	*Friction*
Physical (Fixed)						
a (Baseline Deployment)	0.50	0.50	0.50	0.50	0.50	0.50
δ (Discount rate)	0.04	0.04	0.04	0.04	0.04	0.04
ρ (Depreciation)	0.05	0.05	0.05	0.05	0.05	0.05
ϕ (Decay rate)	0.10	0.10	0.10	0.10	0.10	0.10
ω (Inflow)	0.80	0.80	0.80	0.80	0.80	0.80
Structural (Varied)						
κ (Abatement eff.)	0.06	0.06	0.06	**0.10**	**0.03**	0.06
γ (Invest. elasticity)	0.80	0.80	0.80	0.80	0.80	**1.10**
θ (Abatement cost)	2.0	**1.5**	**4.0**	2.0	2.0	2.0
η (Damage weight)	0.02	**0.05**	**0.005**	0.02	0.02	0.02

8.1 Policy Preference and Cost of Direct Abatement

The parameter $\eta > 0$ measures society's aversion to pollution, and $\theta > 0$ scales the cost of direct abatement. Their effects follow directly from the optimal conditions.

Using the costate equation for pollution,

$$\dot{\tilde{\lambda}}_P(t) = (\delta + \phi)\tilde{\lambda}_P(t) + 2\eta P_t,$$

we can write $\tilde{\lambda}_P(t)$ in integral form as

$$\tilde{\lambda}_P(t) = -2\eta \int_t^{\infty} e^{-(\delta+\phi)(s-t)} P_s \, ds.$$

For any given pollution path $\{P_s\}_{s\geq t}$, a higher damage parameter η increases the magnitude of the shadow cost of pollution.

The optimal abatement rule is

$$A_t = -\frac{\tilde{\lambda}_P(t)}{2\theta} = \frac{\eta}{\theta}\int_t^{\infty} e^{-(\delta+\phi)(s-t)} P_s\, ds.$$

Holding the pollution path fixed,

$$\frac{\partial A_t}{\partial \eta} > 0, \qquad \frac{\partial A_t}{\partial \theta} < 0.$$

Stronger pollution aversion (higher η) and lower abatement cost (smaller θ) therefore raise abatement effort along the entire transition.

In the long run, η and θ jointly determine the steady state pollution stock. Using

$$A^* = \frac{\eta}{\theta(\delta+\phi)} P^*, \qquad P^* = \frac{\omega - \kappa K^*}{\phi + \dfrac{\eta}{\theta(\delta+\phi)}},$$

we obtain, for a given K^*,

$$\frac{\partial A^*}{\partial \eta} > 0, \qquad \frac{\partial A^*}{\partial \theta} < 0, \qquad \frac{\partial P^*}{\partial \eta} < 0, \qquad \frac{\partial P^*}{\partial \theta} > 0.$$

A regime with larger η and smaller θ thus supports a lower steady state pollution stock and a higher steady state abatement level.

These changes also feed back into the capital sector. The costate equation for K_t is

$$\dot{\tilde{\lambda}}_K(t) = (\delta+\rho)\tilde{\lambda}_K(t) - R\kappa + \kappa i_t - \frac{c_0 u_t}{(1+K_t)^2} + \kappa\tilde{\lambda}_P(t),$$

and in steady state we can write

$$\tilde{\lambda}_K^* = \frac{R\kappa - \kappa i^* + \dfrac{c_0 u^*}{(1+K^*)^2} - \kappa\tilde{\lambda}_P^*}{\delta+\rho}, \qquad \tilde{\lambda}_P^* = -\frac{2\eta}{\delta+\phi} P^*.$$

A larger η (and, through a lower P^*, a smaller θ) makes $\tilde{\lambda}_P^*$ more negative, so $-\kappa\tilde{\lambda}_P^*$ increases and the shadow value $\tilde{\lambda}_K^*$ rises. Via the subsidy FOC, this higher shadow value implies larger optimal subsidies i_t, higher green investment u_t, and a larger steady state capital stock K^*.

The simulations in Figure 5 confirm this mechanism: relative to the baseline (S1), the high preference scenario S2 converges to a much greener steady state, while the weak preference scenario S3 ends up with high pollution and only modest deployment.

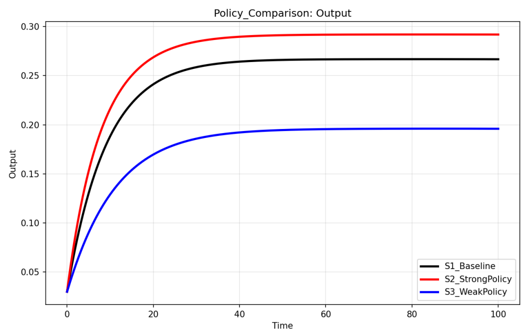

(a) Output

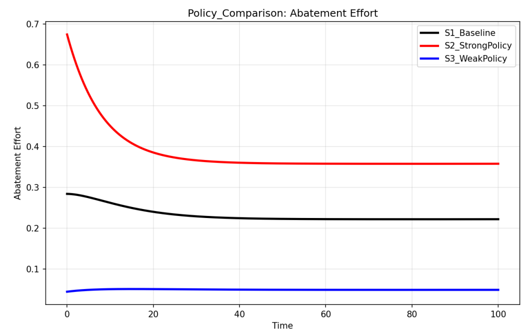

(b) Abatement Effort

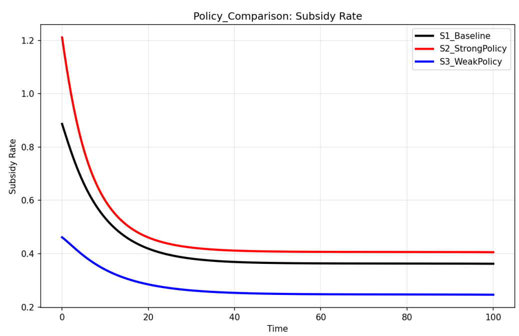

(c) Subsidy Rate

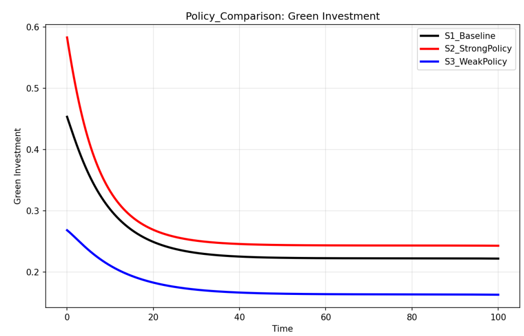

(d) Green Investment

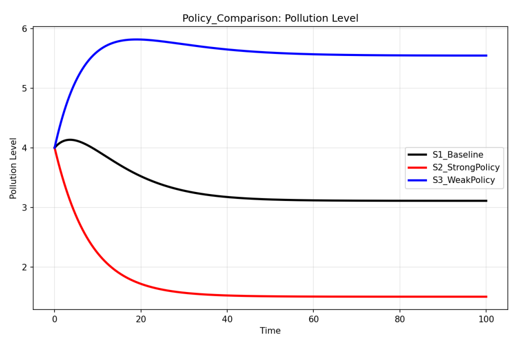

(e) Pollution Level

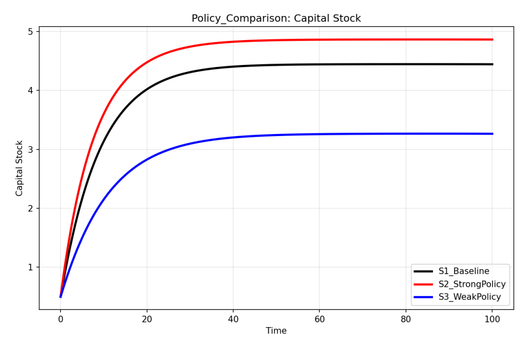

(f) Capital Stock

Figure 5: Policy comparison across three scenarios.

8.2 Deployment Effectiveness and Grid Absorption

The parameter $\kappa > 0$ measures how effective installed solar capital is in generating output and reducing pollution. It enters both the state dynamics and the instantaneous payoff:

$$Q_t = \kappa K_t, \qquad \dot{P}_t = \omega - \phi P_t - \kappa K_t - A_t,$$

$$\pi_t = R\kappa K_t - i_t \kappa K_t - \eta P_t^2 - \beta u_t^2 - \frac{c_0}{1+K_t} u_t - \theta A_t^2.$$

A higher κ raises the marginal revenue of capital and strengthens the automatic pollution reduction via $-\kappa K_t$.

The pollution costate $\tilde{\lambda}_P(t)$ does not depend on κ directly, but κ affects it through the pollution path. A larger κ makes the term $-\kappa K_s$ in $\dot{P}_s$ more powerful, which lowers the future pollution trajectory and makes $\tilde{\lambda}_P(t)$ less negative. Through the abatement rule $A_t = -\tilde{\lambda}_P(t)/(2\theta)$, higher κ therefore reduces optimal abatement along the transition.

For the capital costate we can write

$$\dot{\tilde{\lambda}}_K(t) = (\delta + \rho)\tilde{\lambda}_K(t) - R\kappa + \kappa i_t - \frac{c_0 u_t}{(1+K_t)^2} + \kappa \tilde{\lambda}_P(t),$$

and, in integral form,

$$\tilde{\lambda}_K(t) = \int_t^\infty e^{-(\delta+\rho)(s-t)} \left[R\kappa - \kappa i_s + \frac{c_0 u_s}{(1+K_s)^2} - \kappa \tilde{\lambda}_P(s) \right] ds.$$

Differentiating with respect to κ shows that, as long as the combined term $R - i_s - \tilde{\lambda}_P(s)$ is positive on most of the path, a higher κ raises $\tilde{\lambda}_K(t)$.

The subsidy choice satisfies

$$\tilde{\lambda}_K(t) = \frac{\kappa K_t}{a\gamma i_t^{\gamma-1}} + 2\beta a i_t^\gamma + \frac{c_0}{1+K_t},$$

so for a given K_t a higher $\tilde{\lambda}_K(t)$ implies a larger i_t and thus a larger $u_t = a i_t^\gamma$. In other words, when each unit of capital is more effective, the planner has a stronger incentive to subsidize installation and rely on capital driven pollution reduction rather than on direct abatement.

In steady state, with $u^* = \rho K^*$, the pollution stock is

$$P^*(\kappa, K^*) = \frac{\omega - \kappa K^*}{\phi + \dfrac{\eta}{\theta(\delta + \phi)}}.$$

Holding K^* fixed,

$$\frac{\partial P^*}{\partial \kappa} = -\frac{K^*}{\phi + \dfrac{\eta}{\theta(\delta + \phi)}} < 0, \qquad \frac{\partial A^*}{\partial \kappa} = \frac{\eta}{\theta(\delta + \phi)} \frac{\partial P^*}{\partial \kappa} < 0.$$

For a given capital stock, a higher κ therefore reduces both the steady state pollution level and steady state abatement, because the system can now rely more on the built capital stock to clean the environment. The simulations in Figure 6 show that, in our calibrated parameter range, a higher κ also raises the steady state capital stock itself (Scenario S4 with $\kappa = 0.10$) relative to the low efficiency case (Scenario S5 with $\kappa = 0.03$), so the economy converges to a state with more renewable capacity, lower pollution, and less direct abatement.

The simulation results imply that the planner should pay close attention to the effectiveness of installed solar capacity. Issues such as grid curtailment can be captured by parameter κ.

8.3 Market Frictions and Investment Elasticity

Finally, the parameter $\gamma > 0$ controls how strongly investment responds to the subsidy rate. It links the policy instrument and the physical installation flow through

$$u_t = a i_t^{\gamma}.$$

Higher γ corresponds to a more nonlinear and more convex mapping from subsidies to investment. Unlike η, θ, or κ, the effect of γ on the optimal controls is not globally monotone, because it operates through the marginal fiscal cost of delivering a given u_t rather than directly through benefits or damages.

For given $(K_t, \tilde{\lambda}_K(t))$, subsidy FOC implicitly defines the optimal investment flow $u_t^*(\gamma)$

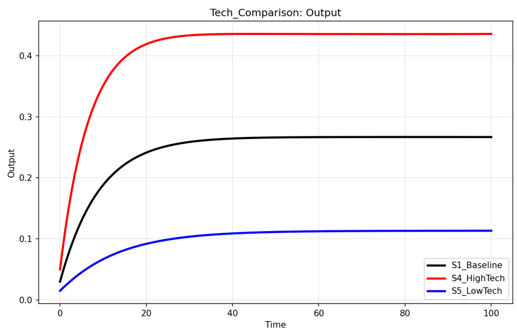

(a) Output

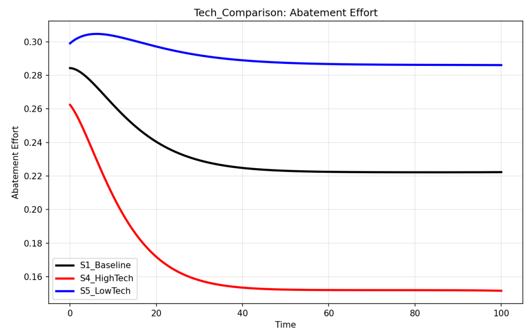

(b) Abatement Effort

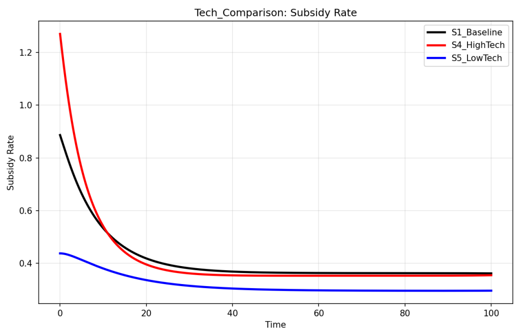

(c) Subsidy Rate

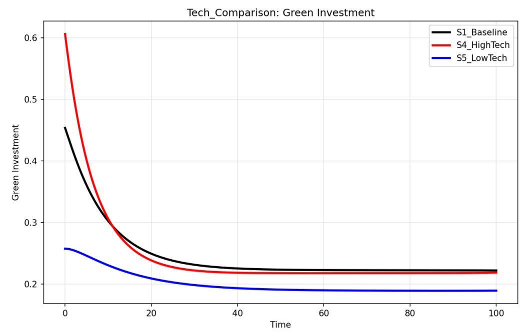

(d) Green Investment

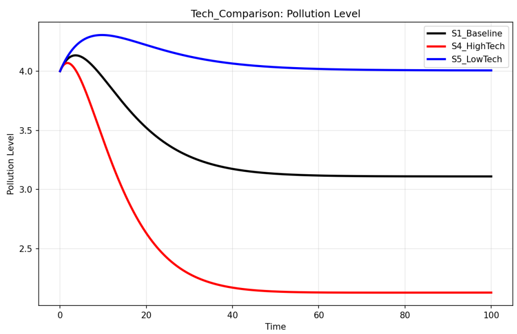

(e) Pollution Level

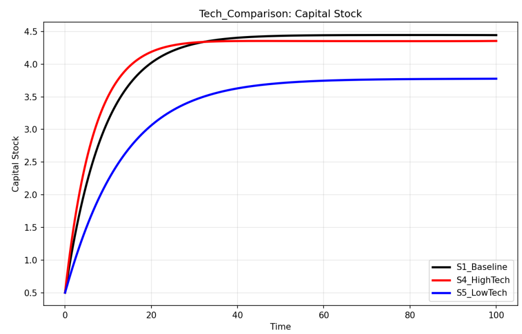

(f) Capital Stock

Figure 6: Efficiency comparison across three scenarios.

as the solution to

$$2\beta u_t + \frac{c_0}{1+K_t} + \frac{\kappa K_t}{\gamma}\, a^{-1/\gamma} u_t^{1/\gamma-1} = \tilde{\lambda}_K(t).$$

The last term is the fiscal component of the marginal cost of investment, and it is the only part that depends on γ. Therefore, let

$$g(u,\gamma) = \frac{\kappa K}{\gamma}\, a^{-1/\gamma} u^{1/\gamma-1}.$$

$$\frac{\partial g}{\partial \gamma} = \frac{\kappa K}{a^{1/\gamma}\gamma^3}\, u^{(1-\gamma)/\gamma}\big(\ln(a/u) - \gamma\big).$$

When $\ln(a/u) - \gamma > 0$, i.e. $u < ae^{-\gamma}$, an increase in γ raises the fiscal marginal cost $g(u,\gamma)$, so the optimal deployment $u_t^*(\gamma)$ decreases locally.

At the same time,

$$i_t = \left(\frac{u_t}{a}\right)^{1/\gamma}$$

if $u_t < a$ implied by $u < ae^{-\gamma}$, then a higher γ means the same u_t requires a higher subsidy rate. Combining these two conditions together, the optimal path in the high friction scenario will lead to a lower u_t and a higher subsidy i_t.

These changes affect the state variables in a straightforward way. With

$$\dot{K}_t = u_t - \rho K_t,$$

a lower u_t path leads to a slower accumulation of capital and a slightly smaller steady state stock K^*. Given

$$\dot{P}_t = \omega - \phi P_t - \kappa K_t - A_t,$$

the weaker capital driven reduction term $-\kappa K_t$ implies a higher pollution path and a slightly larger steady state pollution stock P^*. Through the costate

$$\tilde{\lambda}_P(t) = -2\eta \int_t^\infty e^{-(\delta+\phi)(s-t)} P_s\, ds$$

and the abatement rule $A_t = -\tilde{\lambda}_P(t)/(2\theta)$, this higher pollution path translates into a higher abatement effort throughout the transition.

Figure 7 shows our simulation results. In Scenario 6, we set $a = 0.5$, and raise γ from 0.8 to 1.1. Since $u_t < ae^{-\gamma}$ are satisfied in most time, overall output is mildly affected, but the green transition entails higher fiscal pressure and the economy converges to a steady state where the pollution level is higher.

This pattern is consistent with the early stages of China's DPV poverty alleviation program. Because of limited access to formal credit, and uncertainty about the stability of subsidies, many rural households were reluctant to install rooftop panels. In the model, these frictions show up as a higher γ: subsidies must rise sharply to induce additional investment, generating large fiscal costs but only modest extra capacity. This suggests that rebuilding institutions to reduce frictions and improve the relationship between u_t and i_t is more effective than simply raising subsidy rates, which would be a fiscally expensive and inefficient use of public resources.

9 Extension and Future Plan

While our current framework explains the front-loaded subsidy path, the substitution between the two policy instruments, and the effects of structural environments on the transition path, an important frontier for future research is the integration of stochastic technological uncertainty. In practice, the unit cost of renewable deployment is shaped not only by gradual learning by doing, but also by exogenous breakthroughs such as sudden improvements in photovoltaic efficiency or material science, which can be modeled as Poisson arrival processes. Formally, the unit cost term $\frac{c_0}{1+k_t}$ could jump to $\frac{c_0'}{1+k_t}$, where $c_0 > c_0'$, with some probability at each time t.

Our first prediction is a "waiting effect" induced by technological uncertainty. When a reduction in the initial unit cost c_0 is expected in the near future, the optimal policy may shift toward delaying investment to avoid locking in expensive capital. However, we expect this waiting effect to be state dependent. When the initial pollution stock P_0 is critically high ($P_0 \gg 0$), the catastrophic marginal damage of current emissions is likely to dominate the financial incentive to wait. In this case, the optimal path changes: technological uncertainty

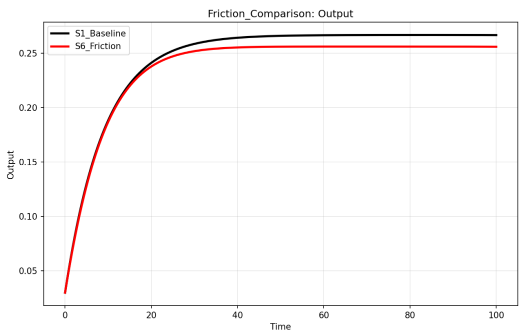

(a) Output

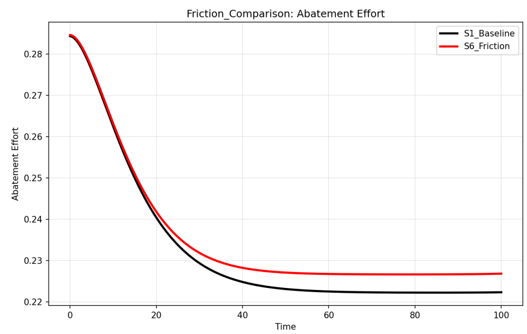

(b) Abatement Effort

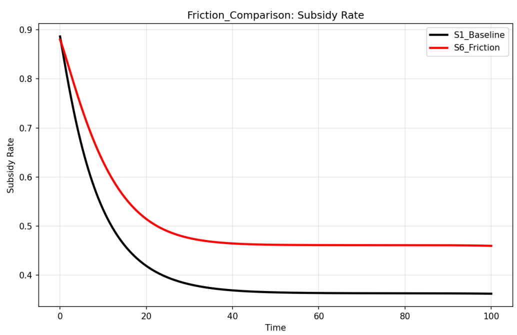

(c) Subsidy Rate

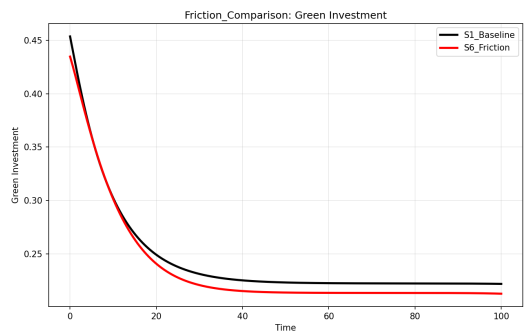

(d) Green Investment

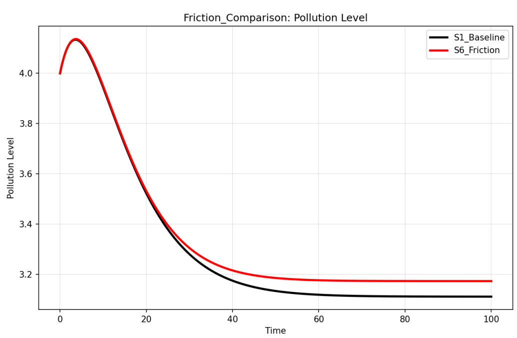

(e) Pollution Level

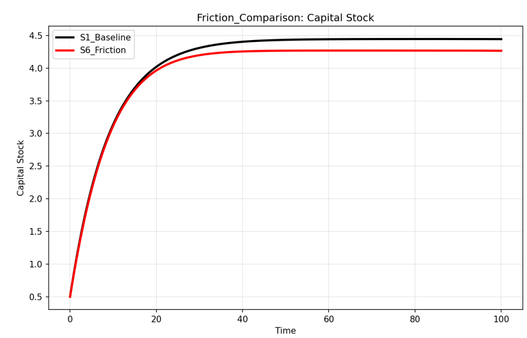

(f) Capital Stock

Figure 7: Market frictions comparison across two scenarios.

substantially delays investment when environmental risk is moderate, but becomes largely irrelevant once the economy faces an ecological emergency.

10 Conclusion

This project develops a continuous-time optimal control framework in which a social planner chooses the joint path of renewable subsidies and direct abatement, considering different types of deployment costs, the future fiscal burden and the pollution dynamics.

Within this framework, we rationalize the front-loaded subsidy pattern observed in China's DPV poverty alleviation program. The government sets a high initial subsidy to accelerate cost reductions through learning by doing, and then gradually phases out the subsidy as fiscal costs rise and the marginal value of additional capital falls. We also study the interaction between the two policy instruments. Although at each instant t the planner chooses the subsidy and direct abatement independently, based on their respective shadow prices, a high early subsidy builds up renewable capital and thereby reduces the need for direct abatement at later stages. We derive the optimal substitution rate between the two instruments in the steady state, but this rate is primarily useful for comparative statics. If the government were to adjust the controls in response to it, the system would no longer remain at the steady state.

We then examine how the transition path responds to changes in key structural parameters. A more pollution-averse government chooses a higher subsidy and converges to a greener equilibrium characterized by higher capital, higher abatement effort, a higher long run subsidy rate, and a lower pollution stock. At the same time, we identify two scenarios in which high subsidies do not necessarily reduce pollution. First, when the effective efficiency of solar power is low, for example due to severe grid curtailment, the planner may optimally scale back subsidies and rely more on direct abatement. Second, when institutional frictions weaken the link between the subsidy rate and actual deployment, higher subsidies simply absorb more public resources without generating commensurate environmental gains, leading to inefficient use of fiscal resources.

Finally, we mention a natural extension that introduces stochastic technological progress.

This extension would allow us to study how technology uncertainty generates waiting incentives and how those incentives interact with environmental risk.

Overall, the project provides a coherent justification for front-loaded renewable subsidies, while highlighting that their effectiveness hinges on government preference, grid conditions, and institutional design. Well-designed subsidy policies must therefore be complemented by improvements in grid integration and implementation capacity, rather than relying on subsidies alone to drive the transition.

References

Chakravorty, U., Roumasset, J., and Tse, K. (1997). Endogenous substitution among energy resources and global warming. *Journal of Political Economy*, 105(6):1201–1234.

Hagspiel, V., Nunes, C., Oliveira, C., and Portela, M. (2021). Green investment under time-dependent subsidy retraction risk. *Journal of Economic Dynamics and Control*, 126:103936.

Hotelling, H. (1931). The economics of exhaustible resources. *Journal of political Economy*, 39(2):137–175.

Keeler, E., Spence, M., and Zeckhauser, R. (1972). The optimal control of pollution. *Journal of economic theory*, 4(1):19–34.

Li, J., Wang, C., Peng, J., Shuai, J., and Shuai, C. (2025a). Impoverished villagers' solar pv adoption in rural china: A perspective of agent intervention, economic benefit perception and sense of community. *Energy*, 315:134250.

Li, R., Song, H., Zhang, J., and Zhang, J. (2025b). The effects of a multifaceted poverty alleviation program on rural income and household behavior in china. *American Economic Journal: Economic Policy*, 17(2):319–357.

Linnerud, K., Andersson, A. M., and Fleten, S.-E. (2014). Investment timing under uncertain renewable energy policy: An empirical study of small hydropower projects. *Energy*, 78:154–164.

Sendstad, L. H. and Chronopoulos, M. (2020). Sequential investment in renewable energy technologies under policy uncertainty. *Energy Policy*, 137:111152.

Slade, M. E. and Thille, H. (2009). Whither hotelling: tests of the theory of exhaustible resources. *Annu. Rev. Resour. Econ.*, 1(1):239–260.

Wang, Y. and Zhen, J. (2025). Evaluating the economic and environmental impacts of distributed photovoltaic policy: Insights from county-level data in china. *Energy Policy*, 198:114509.

Wu, J., Mi, S., Meng, J., and Yu, N. (2025). Does the residential photovoltaic station programme aid poverty alleviation? evidence from rural china. *Energy Policy*, 200:114538.

A Replication Code

I use Python to run the simulation because it can run 6 simulations simultaneously, and it is very fast. You can download a folder from this link. This folder already includes the Python code and graphs generated. If you run the code, and it will generate a new folder with all the graphs on your desktop, after install all the packages needed.